OPEN

Original article

Nuclear Medicine Communications

Histopathology-validated lesion detection rates of clinically significant prostate cancer with mpMRI, [^{68}Ga]PSMA-11-PET and [^{11}C]Acetate-PET

Kristina Sandgren[a,*], Sara N. Strandberg[b,*], Joakim H. Jonsson[a], Josefine Grefve[a], Angsana Keeratijarut Lindberg[a], Erik Nilsson[a], Anders Bergh[c], Karin Söderkvist[d], Camilla Thellenberg Karlsson[d], Bengt Friedrich[e], Anders Widmark[d], Lennart Blomqvist[f], Vibeke Berg Loegager[g], Jan Axelsson[a], Mattias Ögren[b], Margareta Ögren[b], Tufve Nyholm[a] and Katrine Riklund[b]

Objective **PET/CT and multiparametric MRI (mpMRI) are important diagnostic tools in clinically significant prostate cancer (csPC). The aim of this study was to compare csPC detection rates with [^{68}Ga]PSMA-11-PET (PSMA)-PET, [^{11}C] Acetate (ACE)-PET, and mpMRI with histopathology as reference, to identify the most suitable imaging modalities for subsequent hybrid imaging. An additional aim was to compare inter-reader variability to assess reproducibility.**

Methods **During 2016–2019, all study participants were examined with PSMA-PET/mpMRI and ACE-PET/CT prior to radical prostatectomy. PSMA-PET, ACE-PET and mpMRI were evaluated separately by two observers, and were compared with histopathology-defined csPC. Statistical analyses included two-sided McNemar test and index of specific agreement.**

Results **Fifty-five study participants were included, with 130 histopathological intraprostatic lesions >0.05 cc. Of these, 32% (42/130) were classified as csPC with ISUP grade ≥2 and volume >0.5 cc. PSMA-PET and mpMRI showed no difference in performance ($P = 0.48$), with mean csPC detection rate of 70% (29.5/42) and 74% (31/42), respectively, while with ACE-PET the mean csPC detection rate was 37% (15.5/42). Interobserver agreement was higher with PSMA-PET compared to mpMRI [79% (26/33) vs 67% (24/38)]. Including all detected lesions from each pair of observers, the detection rate increased to 90% (38/42) with mpMRI, and 79% (33/42) with PSMA-PET.**

Conclusion **PSMA-PET and mpMRI showed high csPC detection rates and superior performance compared to ACE-PET. The interobserver agreement indicates higher reproducibility with PSMA-PET. The combined result of all observers in both PSMA-PET and mpMRI showed the highest detection rate, suggesting an added value of a hybrid imaging approach.** ***Nucl Med Commun*** **44: 997–1004**

Nuclear Medicine Communications 2023, **44**:997–1004

Keywords: acetate-PET, detection rate, intraprostatic lesion, multiparametric MRI, prostate cancer, PSMA-PET

[a]Department of Radiation Sciences, Radiation Physics, Umea University, [b]Department of Radiation Sciences, Diagnostic Radiology, Umea University, [c]Department of Medical Biosciences, Pathology, Umea University, [d]Department of Radiation Sciences, Oncology, Umea University, [e]Department of Surgical and Perioperative Sciences, Urology and Andrology, Umea University, Umea, [f]Department of Molecular Medicine and Surgery, Karolinska Institute, Solna, Sweden and [g]Department of Radiology, Copenhagen University Hospital in Herlev, Herlev, Denmark

Correspondence to Kristina Sandgren, PhD, Institution of Radiation sciences Umea University, 901 87 Umeå, Sweden
Tel: +46 72 2323217; e-mail: Kristina.sandgren@umu.se

*Kristina Sandgren and Sara N. Strandberg shared first authorship.
Received 9 June 2023 **Accepted** 28 July 2023.

Introduction

Prostate cancer (PC) is the second most common cancer in men worldwide [1]. PC has a wide spectrum of clinical significance and morbidity, and clinical management depends on the histopathological grade, localization and stage [2]. According to European Association of Urology guidelines [3] clinically significant PC (csPC) can be defined as a lesion with histopathological International Society of Urological Pathology (ISUP) grade ≥2. Multiparametric MRI (mpMRI) is used to detect csPC and is currently the imaging modality of choice for T-staging [4] and for targeted biopsy guidance [5]. Currently trending in radiotherapy, focal boosting based on MRI tumor delineation has been shown to improve biochemical recurrence-free survival [6]. The Prostate Imaging Reporting and Data System (PI-RADS) v2.1 is

Supplemental Digital Content is available for this article. Direct URL citations appear in the printed text and are provided in the HTML and PDF versions of this article on the journal's website, www.nuclearmedicinecomm.com.

used for standardized interpretation and reporting of PC MRI [7]. Lesion size and grade are important determinants of lesion detection rates. Turkbey *et al*. [8]. found a sensitivity of 68% with mpMRI for detection of lesions >5 mm diameter, and only 37% for lesions <0.5 mm.

PET/CT with prostate-specific membrane antigen (PSMA) ligands is used mainly for metastasis assessment [9]. PSMA is a membrane-bound zinc protease, with frequent overexpression in PC [10]. Several guidelines for evaluation of PSMA-PET have been proposed, such as the PSMA-RADS and PROMISE classifications [11–13]. Furthermore, early results of PSMA-PET-based gross tumor volume delineation in radiotherapy planning indicate no difference in performance compared to mpMRI [14]. Comparing the performance of mpMRI and PSMA-PET in intraprostatic tumor detection, PSMA-PET has showed a sensitivity of 84% compared to 69% with mpMRI [15]. Other studies confirm the high detection rate of PSMA-PET in the setting of targeted biopsy guidance [16,17].

Before integration into clinical management, histopathological verification is vital. Although other authors have previously compared PSMA-PET and mpMRI to histopathology [15], to our knowledge no such evaluations have been performed with simultaneously acquired PET/MRI data. The aim of this study was to evaluate and compare PSMA-PET, ACE-PET and mpMRI in detection of intraprostatic lesions in primary intermediate and high-risk PC, with co-registered whole-mount histopathology as reference standard.

Materials and methods

Study protocol

This prospective trial was approved by the Swedish medical products agency, the Regional Ethics Board, and the Radiation Protection Committee at Umea University Hospital (EudraCT number: 2015-005046-55, DNR: 2016-220-31M). Consecutive patients matching the inclusion criteria, residing in Vasterbotten County, and referred to Umea University Hospital, were offered to participate. Written informed consent was obtained from each study participant.

Inclusion criteria were intermediate or high-risk PC scheduled for radical prostatectomy, ISUP grade ≥2, ≥2 months since last prostate biopsy, and age >18 years. Exclusion criteria were non-MRI compatible implants, impaired renal function, WHO Performance Status >1, previous neoadjuvant/concomitant medical or surgical castration, transurethral prostate resection <6 months, metastatic PC (based on the study-related imaging modalities), creatinine clearance <30 ml/min, and other known malignancy (except basal cell carcinoma of the skin, or progression-free survival >10 years after previous malignancy).

All participants were examined with ACE-PET/CT and PSMA-PET/mpMRI prior to robot-assisted laparoscopic radical prostatectomy.

PET/CT protocol

Standard ACE-PET/CT protocol was applied. The PET/CT examinations were acquired with a GE Discovery 690 PET/CT scanner (General Electric, Waukesha, Wisconsin, USA). ACE 4–6 MBq/kg was intravenously administered. Ten minutes post-injection, PET data were acquired in time-of-flight mode with 2 min/bed position, from the proximal femur to the head, with 50 cm field-of-view for both PET and the diagnostic non-contrast-enhanced CT. PET data was reconstructed with two different iterative reconstruction algorithms, VuePoint HD, and SharpIR (General Electric). In-plane resolution and slice thickness of the PET and CT scans are presented in Table 1.

PET/MRI protocol

[^{68}Ga]PSMA-11 2 MBq/kg was intravenously administered 60 min post-injection, simultaneous PET/MRI with one pelvic bed position was acquired with a GE Signa 3T PET/MRI scanner (General Electric). The MRI protocol included three-plane (transversal, coronal and sagittal) T2-weighted sequences, a transaxial T1-weighted sequence, diffusion-weighted imaging with b = 0, 200, and 1000 s/mm^2, and a dynamic contrast-enhanced [Gadoteric acid (Dotarem Guerbet, Villepinte, France), 279.3 mg/ml, 15 ml] sequence with acquisition time of 9.6 s repeated for 8 min. Based on the diffusion-weighted imaging an apparent diffusion coefficient map was generated by the MRI scanner software. MRI-sequence characteristics are presented in Supplement 2, Supplemental digital content 1, *http://links.lww.com/NMC/A255*.

Table 1 Demographics and post-surgery characteristics of the 55 included study participants

Characteristics	Median (min–max)
Age (years)	63 (45–76)
PSA (ng/ml)	6.3 (2.9–13.3)
Days between imaging and surgery	26 (2–138)
Injected activity PSMA (MBq)	163 (121–201)
Injected activity ACE (MBq)	426 (286–544)
Post RP ISUP	N (%)
2	29 (52.7%)
3	17 (30.9%)
4	5 (9.1%)
5	4 (7.3%)
pT status	
T2	24 (43.5%)
T3	31 (56.5%)
pN status	
Not removed	44 (80.0%)
Lymph nodes removed without metastasis	9 (16.4%)
Lymph nodes removed with metastasis	2 (3.6%)
Surgical margin	
Positive	14 (24.5%)
Negative	41 (74.5%)
Seminal vesicle involvement	
None	51 (92.7%)
Right	0 (0%)
Left	2 (3.6%)
Both	2 (3.6%)

N, number of patients.

During the MRI session, a 41-minute static PSMA-PET acquisition was collected and reconstructed with SharpIR (General Electric). PET and CT resolution characteristics are presented in Supplement 1, Supplemental digital content 2, *http://links.lww.com/NMC/A256*.

CT background for PSMA-PET reading

For the PSMA-PET/CT evaluation, the CT scan acquired with the ACE-PET/CT was deformably registered to a transversal large field-of-view T2W MRI sequence, acquired with the PSMA-PET/mpMRI, and used as an anatomical synthetic CT (sCT) background to enable comparative reading of the PSMA-PET.

Imaging evaluation

The readers were blinded to clinical information except inclusion criteria. Two MRI radiologists (L.B. and V.B.) evaluated mpMRI separately according to PI-RADS v2.1 [7] in the web-based DICOM viewer and reporting system Collective Minds Radiology ABs platform. Two double-licensed nuclear medicine physicians/radiologists (S.S. and K.R.) evaluated the SharpIR reconstructions of both PSMA-PET/sCT and ACE-PET/CT separately in GE Advanced Workstation Server (AWS; General Electric), and reported maximum and mean standardized uptake values, functional tumor volume, miTNM stage based on molecular imaging, and localization according to the PI-RADS v2.1 sector map [7]. PSMA-PET/sCT was also assessed according to PROMISE and PSMA-RADS [18] European Association of Nuclear Medicine E-PSMA guidelines for standardized reporting [12].

Histopathology

The size and ISUP grade were digitally annotated using NDP.view2 (Hamamatsu Photonic K.K., Hamamatsu City, Japan). In the next step, histopathology was registered to in-vivo MRI according to a previously presented method based on individual 3D-printed prostate molds, ex-vivo MRI and image registrations [19], with the addition of an updated deformable registration including a regularization to preserve relative histopathological distances [20]. All registrations were done in MICE toolkit [21]. After registration, lesions connected in the z-direction (the same in-plane area but located in sequenced histopathology slices) were considered as one lesion.

Statistical analysis

Sample size was determined by assuming a detection rate of 70% for the individual imaging modalities. To achieve 80% power with a significance level of 5%, 67 lesions were required to detect an increase in the combined detection rate to 91% assuming independence between the modalities.

The detection rates of the different imaging modalities were evaluated in a lesion-based analysis and were stratified into different ISUP grades and volumes (>0.5 cc, >0.1 cc, >0.05 cc), and combinations of those. The two-sided McNemar test was used to evaluate differences in detection rates, with a level of significance of $P < 0.05$. Interobserver reliability was assessed using the index of specific agreement and the proportions of agreement of true-positive and false-positive lesions [22].

Results

Fifty-five consecutive study participants were included in the study, as illustrated in the STARD diagram of participant flow in Fig. 1. Patient demographics are presented in Table 1. The median time between imaging and surgery was 26 days (range 2–138). The PET/CT and PET/MRI examinations were performed on the same day in most cases (49/55). The remaining six patients were examined with a maximum 1 month interval. Figure 2 illustrates the imaging modalities compared to histopathology in four of the study participants.

Histopathology revealed 130 lesions >0.05 cc (52 patients), 88 lesions >0.1 cc (50 patients) and 43 lesions >0.5 cc (39 patients). The median volume of lesions >0.5 cc was 1.1 cc (0.5–10.8 cc). The distribution of ISUP grades and lesion volumes are presented in Fig. 3.

Mean detection rates for specific ISUP grades separated by different volume thresholds (>0.05 cc, >0.1 cc and >0.5 cc) are presented in Table 2. The mean detection rates of csPC lesions (ISUP grade ≥2) between each observer pair, for each modality, calculated with varying volume thresholds (>0.05 cc, >0.1 cc and >0.5 cc) are shown in Fig. 4.

Detection rate of csPC lesions >0.5 cc

For the csPC lesions >0.5 cc (42 lesions) the mean observer detection rates for mpMRI, PSMA-PET, and ACE-PET were 74% (31/42), 70% (29.5/42), and 37% (15.5/42), respectively. For these lesions, the joint detection rate (lesions detected by at least one observer) was 90% (38/42) for mpMRI, 79% (33/42) for PSMA-PET and 62% (26/42) for ACE-PET. Supplement 3, Supplemental digital content 3, *http://links.lww.com/NMC/A257* shows a stacked bar plot of the detection frequencies of all modalities and observers.

Detection rate of csPC lesions >0.1 cc

The detection rates of all ISUP grade ≥2 lesions >0.1 cc (74 lesions) for mpMRI, PSMA-PET, and ACE-PET were 65% (48/74), 59% (44/74), and 38% (28/74), respectively.

In the volume range between 0.1–0.5 cc, 32 lesions csPC lesions (ISUP grade ≥2) were found and at least one PSMA-PET observer found 34% (11/32) of these, compared to 31% (10/32) with mpMRI, and 9% (3/32) with ACE-PET.

Fig. 1

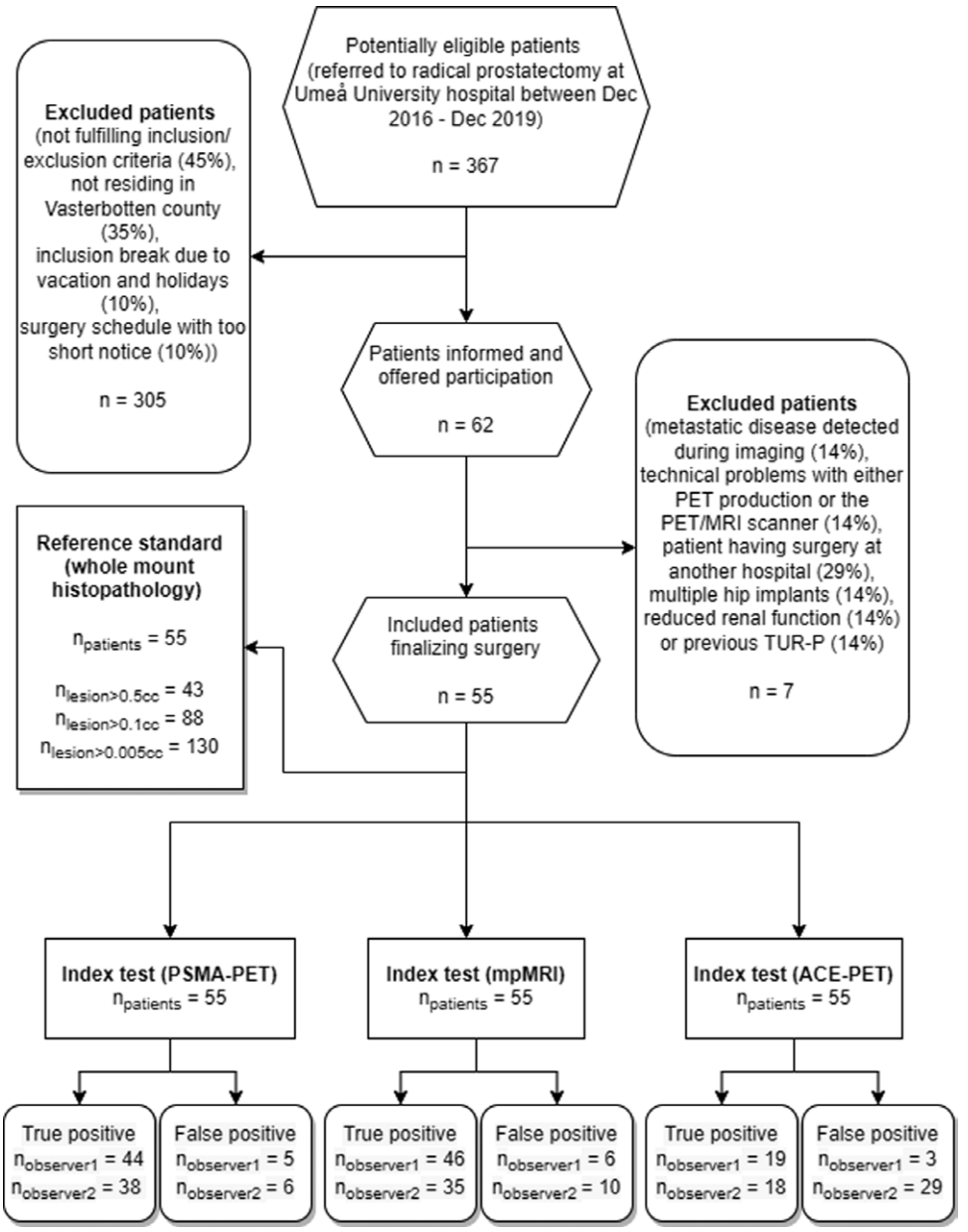

STARD diagram of study participant flow.

Detection rate depending on anatomical location

Among all lesions >0.1 cc, 89% (78/88) were to some extent located in the peripheral zone. Of the 11% (10/88) that were not, PSMA-PET detected 40% (4/10) and mpMRI 20% (2/10). The anatomical location of these 10 lesions were the central zone, transition zone, and the anterior fibromuscular stroma. Their median volume was 0.2 cc.

Joint detection rate of combined modalities

By combining the results of one of the mpMRI observers with one of the PSMA-PET observers, a hybrid PSMA-PET/MRI evaluation can be mimicked. The resulting mean detection rate of csPC lesions >0.5 cc was 89% (37.75/42) [range: 79–93% (33/42–39/42)]. The joint detection rate for all four observers (lesions detected by at least one mpMRI or PSMA-PET observer) was 95% (40/42), with only two lesions undetected. Adding ACE, one more lesion was found, resulting in a detection rate of 98% (41/42).

For the csPC lesions >0.1 cc the mean detection rate for one mpMRI observer and one PSMA-PET observer was 64% (47/74) [range: 57–70% (42/74–52/74)]. The joint detection rate of all csPC lesions >0.1 cc for all observers (both mpMRI and both PSMA) was 77% (56/74). With the

Fig. 2

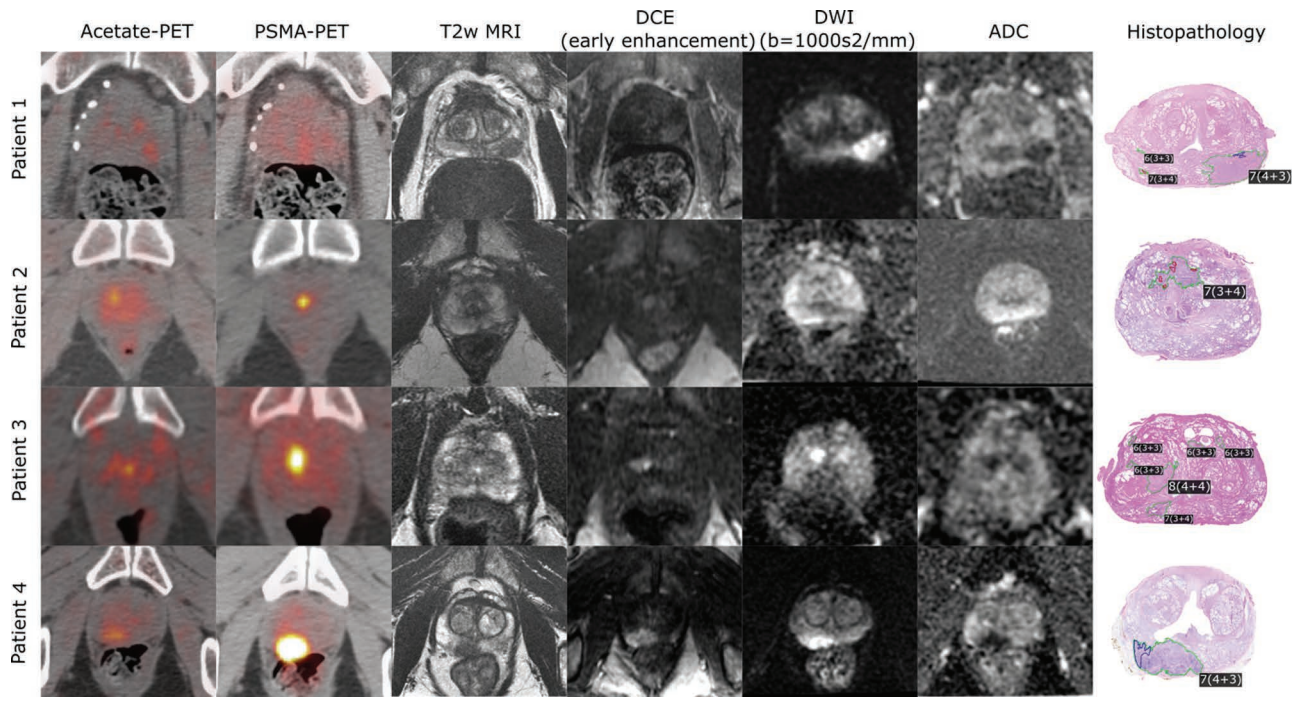

Images from four study participants examined with ACE-PET/CT, PSMA-PET/sCT (both with PET intensity threshold SUV = 10) and mpMRI including a T2-weighted sequence, early dynamic contrast-enhancement, diffusion-weighted sequence (b = 1000 s/mm^2), and apparent diffusion coefficient map. In our first example (case 1) all modalities (both observers), except for PSMA-PET, correctly identified the dominant intraprostatic lesion. In case 2, the dominant lesion was correctly identified by both PSMA-PET observers, while mpMRI and ACE-PET were read as negative. In case 3, both PSMA-PET observers, and one mpMRI observer detected the dominant lesion. Lastly, in case 4, all modalities were in agreement and all observers detected the lesion.

addition of ACE, 80% (59/74) lesions were detected. In total, three PSMA-negative lesions were positive and identified on ACE (2 with ISUP grade ≥2 and one with ISUP grade 1).

False-positive findings

The average number of false positive lesions was 16 (range: 3–29) for ACE-PET, 8 (range: 6–10) for mpMRI and 6 (range: 5–6) for PSMA-PET. The total number of false positive lesions, reported by at least one observer, was 30 for ACE-PET, 13 for mpMRI and 8 for PSMA-PET, respectively.

McNemar test

In the evaluation of lesion detection >0.1 cc, the McNemar test showed no significant difference (P = 0.48) in diagnostic performance between mpMRI and PSMA-PET. However, the diagnostic performance of ACE-PET was significantly lower compared to mpMRI and PSMA-PET (P = 0.001 and 0.002, respectively). Comparing a combined PSMA-PET and mpMRI reading to stand-alone mpMRI and PSMA-PET, the McNemar test showed that the combination of PSMA-PET and mpMRI was superior to the individual modalities mpMRI and PSMA-PET (P = 0.02 and 0.003, respectively).

Interobserver agreement

The index of specific agreement for detection of lesions >0.1 cc was calculated according to the method proposed by Shih *et al.* [22], to 74%, 84%. and 34% for mpMRI, PSMA-PET and ACE-PET, respectively. The proportion of agreement for true positive lesions >0.5 cc was 63% (24/38), 79% (26/33), and 23% (6/26) for mpMRI, PSMA-PET and ACE-PET observers, respectively. The proportion of agreement for false positive lesions was 16% (3/19), 21% (3/14), and 6% (2/34) for the mpMRI, PSMA-PET and ACE-PET observers, respectively. Hence, the PSMA-PET evaluation resulted in fewer lesions only identified by one observer compared to mpMRI.

Discussion

This study compared the diagnostic performance of PSMA-PET, ACE-PET and mpMRI for detection of clinically significant intraprostatic lesions in treatment-naive intermediate and high-risk PC, with histopathological validation. The main result of this study shows that the mean lesion detection rates were similar with mpMRI and PSMA-PET. The joint result of both observers further increased the detection rate, and even more so did the combination of both modalities mpMRI and PSMA-PET, suggesting that a hybrid PSMA-PET/MRI evaluation could improve diagnostic imaging in

Fig. 3

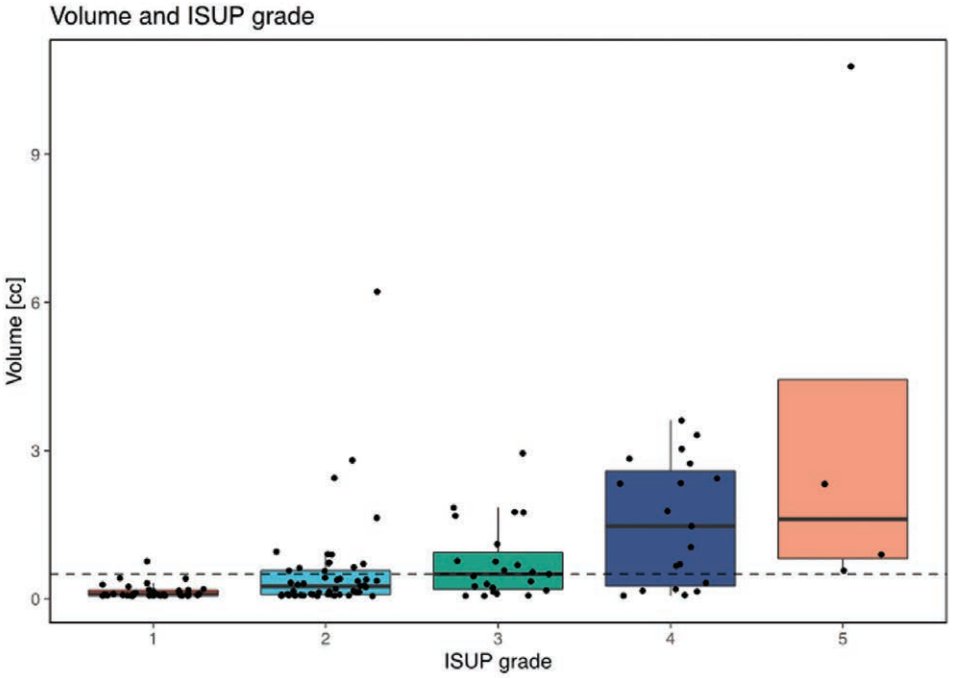

Characteristics of lesions >0.05 cc identified in the histopathological examination (130 lesions). Each box represents the interquartile range with the median value marked with a black line. The black dots represent the individual data points in each ISUP grade. The >0.5 cc threshold is marked with a dashed line (n > 0.5 cc = 43).

Table 2 Mean observer detection rates (%) of intraprostatic lesions based on different ISUP grades and lesion volume thresholds, for the different modalities

Lesions with a volume >0.05 cc					
ISUP grade (N)	1 (34)	2 (50)	3 (23)	4 (19)	5 (4)
ACE	4	10	15	32	63
mpMRI	7	21	52	61	100
PSMA	4	25	54	55	100
Lesions with a volume >0.1 cc					
ISUP grade (N)	1 (14)	2 (33)	3 (20)	4 (17)	5 (4)
ACE	4	15	18	35	63
mpMRI	7	32	60	68	100
PSMA	11	35	60	62	100
Lesions with a volume >0.5 cc					
ISUP grade (N)	1 (1)	2 (14)	3 (11)	4 (13)	5 (4)
ACE	50	29	27	46	63
mpMRI	0	54	82	81	100
PSMA	0	61	68	73	100

N, number of lesions.

csPC. The interobserver index of specific agreement was higher with PSMA-PET than with mpMRI (84% compared to 74%), indicating that PSMA-PET might be less observer-dependent and easier to reproduce. As expected, ACE-PET was inferior in this setting, given that ACE uptake overlaps in benign prostatic hyperplasia and PC [23]. The rationale for including ACE-PET in this study with focus on the primary tumor, was to explore the possible associations between different radiotracer uptakes and mpMRI signal patterns, and different histopathological properties within the primary tumor; however, this is not within the scope of the present article. Even so, it is worth mentioning that three histology-confirmed csPC lesions were PSMA-PET negative and ACE-PET positive, indicating the usefulness of ACE-PET as a possible problem-solver in selected cases where high suspicion of csPC remains, despite negative PSMA-PET and mpMRI.

Our result with similar performance of PSMA-PET and mpMRI is supported by a recent publication by Sonni *et al*. which demonstrated similar accuracy of mpMRI and PSMA-PET in intraprostatic lesion localization [24]. In contrast, a comparative study by Zamboglou *et al*. in 2021

Fig. 4

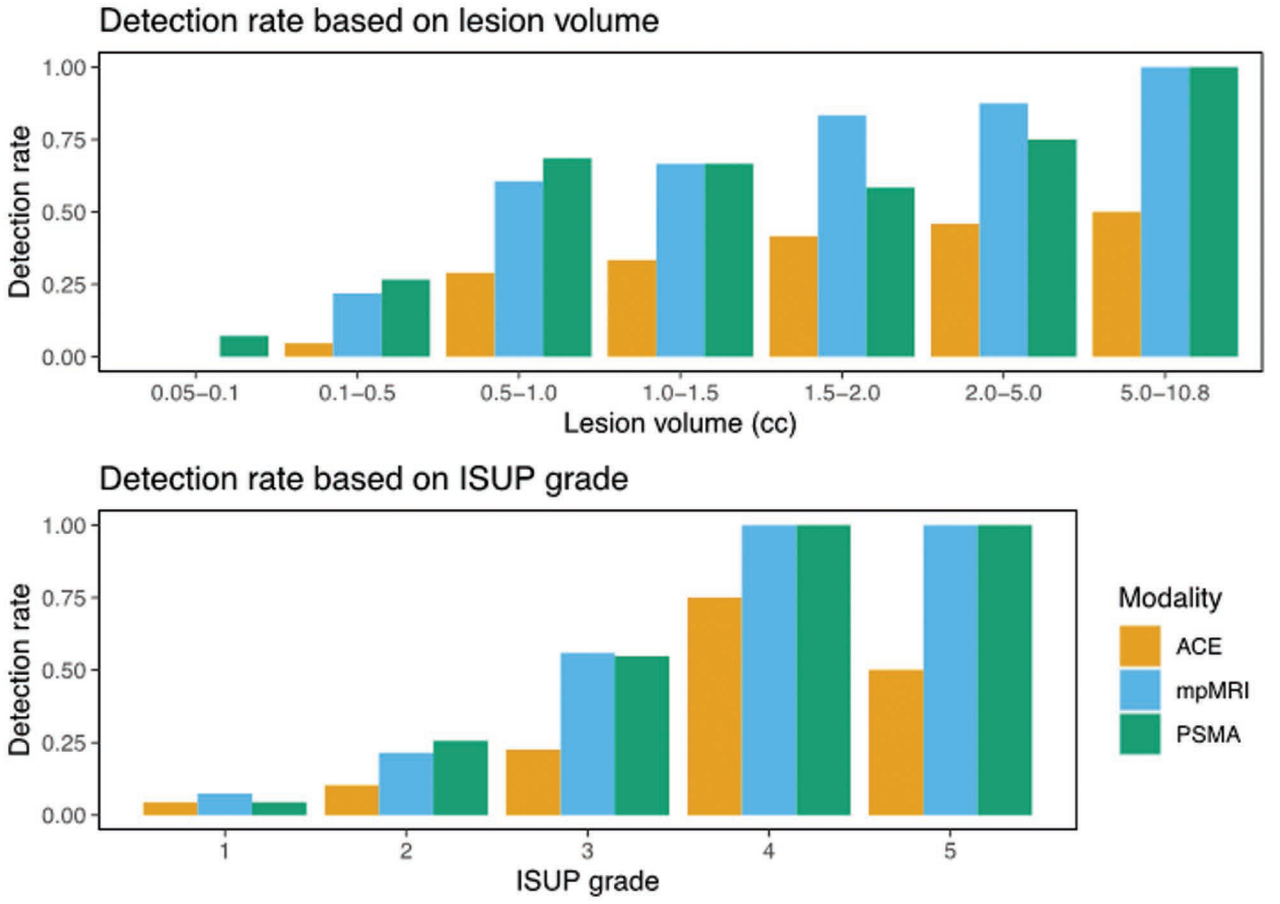

Mean observer detection rate of lesions with ISUP grade ≥2 calculated for each modality and with different lesions volume bins (upper graph), and the mean observer detection rate for each ISUP grade (lower graph).

showed higher sensitivity for intraprostatic tumor detection with PSMA-PET (84%) compared to mpMRI (69%), with whole-mount histopathology and different co-registration methods [15]. However, that study included only ten participants.

In our cohort of 55 patients, only 42 lesions larger than 0.5 cc and ISUP ≥ 2 were found, which was lower than expected when designing the study. When including lesions larger than 0.1 cc, we found 88 lesions and thus performed our statistical significance testing in this extended group.

The indication from our results that the PSMA-PET/MRI hybrid imaging and reporting approach would be preferable, is in line with previous studies [25,26]. Furthermore, the high interobserver agreement with PSMA-PET is well aligned with previous publications stating the highly consistent and reproducible interpretation of PSMA-PET in PC staging performed by observers with high level of experience [27].

One possible interference regarding the interobserver agreement is that both PSMA-PET observers have worked together for many years, while the MRI readers have no such history. Furthermore, previous experience of different MRI protocols, manufacturers and scanners may have affected the mpMRI interobserver agreement. Furthermore, to get an anatomical background without MRI information, the PSMA-PET was evaluated with a sCT, which is associated with a degree of image registration uncertainty. However, the prostate region was minimally affected by this problem, thereby reducing the possible negative effects of this limitation. Also, the ACE-PET/CT protocol was designed without iodine contrast since the PET/MRI and PET/CT examinations were scheduled in close succession, thus further impairing the CT information. According to the ESUR 2018 Guidelines on Contrast Agents v 10.0 [28] injections of iodine- and gadolinium-based contrast may be administered within the same day with an interval of 4 h. This time range, combined with the time required for the PET/MRI examination, was not considered feasible and therefore MRI contrast was prioritized based on its superior diagnostic properties compared to CT contrast in the setting of intraprostatic lesion characterization. Regarding

the mpMRI, the collection of data for this study started in 2016, before PI-RADS v2.1 was implemented and therefore deviates from the current PI-RADS v2.1 recommendation of 3 mm slice thickness of the diffusion-weighted and contrast-enhanced sequences. The slice thickness in the protocol for these sequences was 5 mm, to facilitate correlation with the histopathology sections. This limitation might have impaired mpMRI detection of lesions <5 mm.

Although the present study did not perform a hybrid PSMA-PET/MRI evaluation, our combined result of the different modalities (PSMA-PET and mpMRI) and several other publications have presented data supporting that hybrid PSMA-PET/MRI can improve the diagnosis of csPC compared with mpMRI alone [29], and this will be the focus of our next analysis of the study data. Furthermore, analysis of correlations between different radiotracer uptakes, MRI patterns and histopathologic tumor properties is currently ongoing and will be presented in a separate article.

Conclusion

PSMA-PET and mpMRI showed high detection rates of csPC and no difference in performance. The interobserver agreement indicates higher reproducibility with PSMA-PET. The combined result of all observers in both PSMA-PET and mpMRI showed the highest detection rate, suggesting an added value of a hybrid imaging approach.

Acknowledgements

This project was funded by the Regional Cancer Foundation of Norrland, Umea, Sweden, Cancerfonden, Sweden, and Västerbotten County, Sweden.

Conflicts of interest

There are no conflicts of interest.

References

1 Sung H, Ferlay J, Siegel RL, Laversanne M, Soerjomataram I, Jemal A, *et al.* Global Cancer Statistics 2020: GLOBOCAN estimates of incidence and mortality worldwide for 36 cancers in 185 countries. *CA Cancer J Clin* 2021; **71**:209–249.
2 Fuchsjager M, Shukla-Dave A, Akin O, Barentsz JO, Hricak H. Prostate cancer imaging. *Acta Radiol* 2008; **49**:107–120.
3 Turkbey B, Rosenkrantz AB, Haider MA, Padhani AR, Villeirs G, Macura KJ, *et al.* Prostate imaging reporting and data system version 2.1: 2019 update of prostate imaging reporting and data system version 2. *Eur Urol* 2019; **76**:340–351.
4 Caglic I, Kovac V, Barrett T. Multiparametric MRI - local staging of prostate cancer and beyond. *Radiol Oncol* 2019; **53**:159–170.
5 Ahdoot M, Wilbur AR, Reese SE, Lebastchi AH, Mehralivand S, Gomella PT, *et al.* MRI-Targeted, systematic, and combined biopsy for prostate cancer diagnosis. *N Engl J Med* 2020; **382**:917–928.
6 Kerkmeijer LGW, Groen VH, Pos FJ, Haustermans K, Monninkhof EM, Smeenk RJ, *et al.* Focal boost to the intraprostatic tumor in external beam radiotherapy for patients with localized prostate cancer: results from the FLAME randomized phase III trial. *J Clin Oncol* 2021; **39**:787–796.
7 American College of Radiology. *PI-RADS ® v2.1 PI-RADS ® Prostate Imaging-Reporting and Data System 2019*. Version 2.1 PI-RADS. American College of Radiology; 2019.
8 Turkbey B, Mani H, Shah V, Rastinehad AR, Bernardo M, Pohida T, *et al.* Multiparametric 3T prostate magnetic resonance imaging to detect cancer: Histopathological correlation using prostatectomy specimens processed in customized magnetic resonance imaging based molds. *J Urol* 2011; **186**:1818–1824.
9 Bouchelouche K, Turkbey B, Choyke P, Capala J. Imaging prostate cancer: an update on positron emission tomography and magnetic resonance imaging. *Curr Urol Rep* 2010; **11**:180–190.
10 Bostwick DG, Pacelli A, Blute M, Roche P, Murphy GP. Prostate specific membrane antigen expression in prostatic intraepithelial neoplasia and adenocarcinoma: a study of 184 cases. *Cancer* 1998; **82**:2256–2261.
11 Eiber M, Herrmann K, Calais J, Hadaschihk B, Giesel FL, Hartenbach M, *et al.* PROstate cancer Molecular Imaging Standardized Evaluation (PROMISE): proposed miTNM classification for the interpretation of PSMA-ligand PET/CT. *J Nucl Med* 2017; **117**:198119.
12 Ceci F, Oprea-Lager DE, Emmett L, Adam JA, Bomanji J, Czernin J, *et al.* E-PSMA: the EANM standardized reporting guidelines v1.0 for PSMA-PET. *Eur J Nucl Med Mol Imaging* 2021; **48**:1626–1638.
13 Rowe SP, Pienta KJ, Pomper MG, Gorin MA. Proposal for a structured reporting system for prostate-specific membrane antigen-targeted PET Imaging: PSMA-RADS Version 1.0. *J Nucl Med* 2018; **59**:479–485.
14 Zamboglou C, Drendel V, Jilg CA, Rischke HC, Beck TI, Schultze-Seemann W, *et al.* Comparison of 68Ga-HBED-CC PSMA-PET/CT and multiparametric MRI for gross tumour volume detection in patients with primary prostate cancer based on slice by slice comparison with histopathology. *Theranostics* 2017; **7**:228–237.
15 Zamboglou C, Kramer M, Kiefer S, Bronsert P, Ceci L, Sigle A, *et al.* The impact of the co-registration technique and analysis methodology in comparison studies between advanced imaging modalities and whole-mount-histology reference in primary prostate cancer. *Sci Rep* 2021; **11**:1–10.
16 Liu Y, Yu H, Liu J, Zhang X, Lin M, Schmidt H, *et al.* A pilot study of 18F-DCFPyL PET/CT or PET/MRI and ultrasound fusion targeted prostate biopsy for intra-prostatic PET-positive lesions. *Front Oncol* 2021; **11**:1–9.
17 Zhang L Le, Li WC, Xu Z, Jiang N, Zang SM, Xu LW, *et al.* 68Ga-PSMA PET/CT targeted biopsy for the diagnosis of clinically significant prostate cancer compared with transrectal ultrasound guided biopsy: a prospective randomized single-centre study. *Eur J Nucl Med Mol Imaging* 2021; **48**:483–492.
18 Rowe SP, Pienta KJ, Pomper MG, Gorin MA. Proposal for a structured reporting system for prostate-specific membrane antigen-targeted PET imaging: PSMA-RADS version 1.0. *J Nucl Med* 2018; **59**:479–485.
19 Sandgren K, Nilsson E, Keeratijarut Lindberg A, Strandberg S, Blomqvist L, Bergh A, *et al.* Registration of histopathology to magnetic resonance imaging of prostate cancer. *Phys Imaging Radiat Oncol* 2021; **18**:19–25.
20 Finnegan RN, Reynolds HM, Ebert MA, Sun Y, Holloway L, Sykes JR, *et al.* A statistical, voxelised model of prostate cancer for biologically optimised radiotherapy. *Phys Imaging Radiat Oncol* 2022; **21**:136–145.
21 Nyholm T, Berglund M, Brynolfsson P, Jonsson J. EP-1533: ICE-Studio - an interactive visual research tool for image analysis. *Radiother Oncol* 2015; **115**:S837.
22 Shih JH, Greer MD, Turkbey B. The problems with the kappa statistic as a metric of interobserver agreement on lesion detection using a third-reader approach when locations are not prespecified. *Acad Radiol* 2018; **25**:1325–1332.
23 Kato T, Tsukamoto E, Kuge Y, Takei T, Shiga T, Shinohara N, *et al.* Accumulation of [11C]acetate in normal prostate and benign prostatic hyperplasia: Comparison with prostate cancer. *Eur J Nucl Med* 2002; **29**:1492–1495.
24 Sonni I, Felker ER, Lenis AT, Sisk AE, Bahri S, Allen-Auerbach M, *et al.* Head-to-head comparison of 68Ga-PSMA-11 PET/CT and mpMRI with histopathology gold-standard in the detection, intra-prostatic localization and local extension of primary prostate cancer: results from a prospective single-center imaging trial. *J Nucl Med* 2022; **63**:847–854.
25 Evangelista L, Zucchetta P. PET/ MRI in prostate cancer: a systematic review and meta-analysis. *Eur J Nucl Med Mol Imaging* 2021; **48**:859–873.
26 Arslan A, Karaarslan E, Güner AL, Sağlican Y, Tuna MB, Özişik O, *et al.* Comparison of MRI, PSMA PET/CT, and fusion PSMA PET/MRI for detection of clinically significant prostate cancer. *J Comput Assist Tomogr* 2021; **45**:210–217.
27 Fendler WP, Calais J, Allen-Auerbach M, Bluemel C, Eberhardt N, Emmett L, *et al.* 68Ga-PSMA-11 PET/CT interobserver agreement for prostate cancer assessments: an International Multicenter Prospective Study. *J Nucl Med* 2017; **58**:1617–1623.
28 Contrast Media Safety Committee. ESUR guidelines on contrast agents v10.0. *Eur Soc Urogenit Radiol* 2018:0–45.
29 Fernandes MC, Yildirim O, Woo S H, Vargas A, Hricak H. The role of MRI in prostate cancer: current and future directions. *MAGMA* 2022; **35**:503–521. doi: https://doi.org/10.1007/s10334-022-01006-6.